

SANDIA REPORT

SAND2002-0040

Unlimited Release

Printed January 2002

Low Mass Transmission Lines for Z-Pinch Driven Inertial Fusion

Stephen A. Slutz

Prepared by
Sandia National Laboratories
Albuquerque, New Mexico 87185 and Livermore, California 94550

Sandia is a multiprogram laboratory operated by Sandia Corporation, a Lockheed Martin Company, for the United States Department of Energy under Contract DE-AC04-94AL85000.

Approved for public release; further dissemination unlimited.



Sandia National Laboratories

Issued by Sandia National Laboratories, operated for the United States Department of Energy by Sandia Corporation.

NOTICE: This report was prepared as an account of work sponsored by an agency of the United States Government. Neither the United States Government, nor any agency thereof, nor any of their employees, nor any of their contractors, subcontractors, or their employees, make any warranty, express or implied, or assume any legal liability or responsibility for the accuracy, completeness, or usefulness of any information, apparatus, product, or process disclosed, or represent that its use would not infringe privately owned rights. Reference herein to any specific commercial product, process, or service by trade name, trademark, manufacturer, or otherwise, does not necessarily constitute or imply its endorsement, recommendation, or favoring by the United States Government, any agency thereof, or any of their contractors or subcontractors. The views and opinions expressed herein do not necessarily state or reflect those of the United States Government, any agency thereof, or any of their contractors.

Printed in the United States of America. This report has been reproduced directly from the best available copy.

Available to DOE and DOE contractors from
U.S. Department of Energy
Office of Scientific and Technical Information
P.O. Box 62
Oak Ridge, TN 37831

Telephone: (865)576-8401
Facsimile: (865)576-5728
E-Mail: reports@adonis.osti.gov
Online ordering: <http://www.doe.gov/bridge>

Available to the public from
U.S. Department of Commerce
National Technical Information Service
5285 Port Royal Rd
Springfield, VA 22161

Telephone: (800)553-6847
Facsimile: (703)605-6900
E-Mail: orders@ntis.fedworld.gov
Online order: <http://www.ntis.gov/ordering.htm>



SAND2002-0040
Unlimited Release
Printed January 2002

Low Mass Transmission Lines for Z-Pinch Driven Inertial Fusion

Stephen A. Slutz
Target and Z-Pinch Theory Department

Craig L. Olson
Pulsed Power Science Center

Sandia National Laboratories
P. O. Box 5800
Albuquerque, NM 87185-1186

Per Peterson
University of California
Berkeley, CA

Abstract

Recyclable transmission lines (RTL) are studied as a means of repetitively driving z pinches. The lowest reprocessing costs should be obtained by minimizing the mass of the RTL. Low mass transmission lines (LMTL) could also help reduce the cost of a single shot facility such as the proposed X-1 accelerator and make z-pinch driven space propulsion feasible. We present calculations to determine the minimum LMTL electrode mass to provide sufficient inertia against the magnetic pressure produced by the large currents needed to drive the z pinches. The results indicate an electrode thickness which is much smaller than the resistive skin depth. We have performed experiments to determine if such thin electrodes can efficiently carry the required current. The tests were performed with various thickness of materials. The results indicate that LMTLs should efficiently carry the large z-pinch currents needed for inertial fusion. We also use our results to estimate of the performance of pulsed power driven pulsed nuclear rockets.

acknowledgments

We gratefully acknowledge the experimental support of Dustin Romero and all of the Saturn-crew. The interest and support of Jeff Quintenz, Keith Matzen, and Dillon McDaniel is gratefully acknowledged. This work was performed under and LDRD.

Contents

I. Introduction	6
II. Calculations of minimum LMTL inertial mass	7
III. Low Mass Transmission Line experiments	11
IV. Power flow.....	24
V. Pulsed Nuclear Space Propulsion	31
VI. Summary.....	37
Appendix.....	38
References.....	41

Figures

Fig. 1	A schematic of a Low Mass Transmission Line	9
Fig. 2	A schematic of the experimental design	12
Fig. 3	The experimental set up 3D cutaway	13
Fig. 4	The currents plotted as a function of time for shot 2962	14
Fig. 5	The effective resistance plotted as a function of time for shot 2962	15
Fig. 6	The resistive loss plotted as a function of time for shot 2962.....	16
Fig. 7	The currents plotted as a function of time for shot 2963	16
Fig. 8	The resistance of the 20 μ mylar plotted as a function of time.....	17
Fig. 9	The resistive loss plotted as a function of time for shot 2963.....	18
Fig. 10	The currents plotted as a function of time for shot 2964	19
Fig. 11	The effective resistance as a function of time for shot 2964.....	20
Fig. 12	The resistive energy loss as a function of time for shot 2964.....	20
Fig. 13	The current waveforms as a function of time for shot 2965	21
Fig. 14	The effective resistance as a function of time for shot 2965.....	21
Fig. 15	The resistive energy loss as a function of time for shot 2965.....	22
Fig. 16	The fraction of the current carried by the shunt electrodes	23
Fig. 17	Fraction of the available energy lost to resistance	23
Fig. 18	The calculated minimum angle as a function of α	26
Fig. 19	The LMTL mass plotted as a function of α	27
Fig. 20	The required driving voltage as a function of α	28
Fig. 21	The efficiency is plotted as a function of α	29
Fig. 22	A schematic of a disk electrode	30
Fig. 23	A schematic of a nuclear rocket driven by pulsed power	32
Fig. 24	The transmission line mass as a function of the current risetime	35
Fig. 25	The specific impulse as a function of the current risetime.....	35
Fig. 26	The burn time to reach 30 km/s for a 100 metric ton spacecraft	36
Fig. A1	Schematic of a disk transmission line with an explosive unit.....	38
Fig. A2	The specific impulse coefficient as a function of z_T/r_T	40

I. Introduction

Z-pinches have generated thermal x-rays with high efficiency and thus are a promising driver for inertial fusion. The “Recyclable Transmission Line” (RTL) is a promising means of providing standoff and thus allowing repetitive operation of z-pinch drivers for uses such as generating electrical energy or space propulsion. These RTLs could be formed inexpensively by casting of appropriate materials such as the reactor coolant flibe (Fluorine, Lithium, Beryllium). Since flibe is an insulator, a conducting coating would be required. Preliminary experiments on the Saturn facility indicate that either lead or aluminum could be used. Recent analysis suggest that an alloy of iron/carbon/tungsten would be a better choice for the conducting material. The components of this alloy are inert and immiscible in flibe, and will form a solid precipitate that can be recovered mechanically from the molten flibe by filtering and centrifugation processes. Activation products from these materials have relatively short half lives, so no long-lived radioactive waste would be generated. By maintaining carbon and tungsten concentrations around 1-2% by weight, the iron maintains the properties of steel and can be formed using the same processes used for fabricating sheet-metal components of automobiles, although remote fabrication will be required due to the activity from short-lived activation products.

In this report, we investigate the option of using low mass transmission lines (LMTLs) as a means of reducing the cost of recycling. LMTLs could be used for inertial fusion energy, or to help reduce the cost of a single shot facility high yield facility such as the proposed X-1 accelerator. An additional application is pulsed nuclear space propulsion. LMTLs are critical to this application because the mass of the transmission line will become part of the rocket propellant. Therefore high specific impulses require low mass transmission lines.

Large currents are needed to drive z-pinch inertial fusion. Numerical simulations¹ indicate that a current in excess of 55 MA will be required to drive a capsule with a fusion

yield of 500 MJ. Simple scaling suggests that much higher currents (~ 100 MA) will be required to drive capsules with a yield of several GJ. We shall assume that 100 MA is required although alternate schemes such as the fast ignitor concept could substantially reduce the required drive current. High current generates a very large magnetic pressure, which tends to push the LMTL electrodes apart. This motion is opposed by the inertial mass of the electrodes. The requirement that the gap between the electrodes does not change excessively during the current pulse places a minimum LMTL inertial mass, which is calculated in section II.

It is found that required areal density of the electrodes decreases strongly with radius and the outer portion of the LMTL could be very thin. This minimum electrode thickness can be much smaller than the resistive skin depth of the cold electrode material. This suggests that there might be excessive resistive losses if very thin electrodes are used. However, it is difficult to calculate the magnitude of this effect, due to the complicated nature of surface breakdown phenomenon which can lead to highly conducting plasmas. Experiments were performed to investigate the resistive effects of very thin electrodes. These experiments indicate that 20 μ of mylar is sufficient to carry the current with acceptable resistive losses. This result indicates that a transmission line with a mass as little as 2 kg could be used for energy applications. The experiments are described in section III. Some issues associated with the magnetic insulation of the transmission line are included in the section IV. Ramifications for pulsed nuclear propulsion are discussed in section V and conclusions are drawn in section VI.

II. Calculations of minimum LMTL inertial mass

The RTL option for standoff is to construct a portion of the MITL (Magnetically Insulated Transmission Line) out of material that can be recycled. We wish to minimize the amount of material that is recycled each shot. The magnetic field generated by the current within the transmission line produces a pressure which pushes the electrodes apart. This

pressure is typically much higher than the material strength of the electrode materials so the electrodes will accelerate away from each other during the current pulse. This outward motion of the electrodes increases the inductance of the transmission line making it more difficult to deliver the high currents required by the z pinch. Assuming thin electrodes, the movement is determined by Newton's Eq.

$$F = \frac{B^2}{2\mu_0}A = M\frac{d^2x}{dt^2} \quad (1)$$

where x is the displacement of the electrodes and the magnetic field is determined by the relation $B = \frac{\mu_0 I}{2\pi r}$. The current profile produced by pulsed power accelerators such as Z can be approximated by the formula

$$I = I_p \left(\frac{3\sqrt{3}}{2} \right)^{1/2} \tau \sqrt{1 - \tau^4} \quad (2)$$

where I_p is the peak current, $\tau = t/t_p$ and t_p is total current pulse length. This form admits an analytic solution to the z-pinch implosion², which we shall find useful. Equations (1) and (2) yield the result

$$x = \frac{11\sqrt{3}}{224\pi\Gamma(r)} \left(\frac{\mu_0}{4\pi} \right) \left(\frac{I_p t_p}{r} \right)^2 \quad (3)$$

where $\Gamma(r)$ is the areal density (kg/m^2) of the electrodes. As can be seen from Eq. (3), the electrode motion is limited by the areal density (thickness) of the electrodes. Thus the acceptable amount of electrode motion determines the minimum areal density of the electrodes and hence the total mass of the transmission lines.

The electrode motion needs to be limited to a small fraction, Δg , of the transmission line gap, g . Low mass electrodes will have little shear strength. This limits the transmission line geometry to conics, which can be supported by tensile strength alone. An example of this geometry is shown in Fig. 1

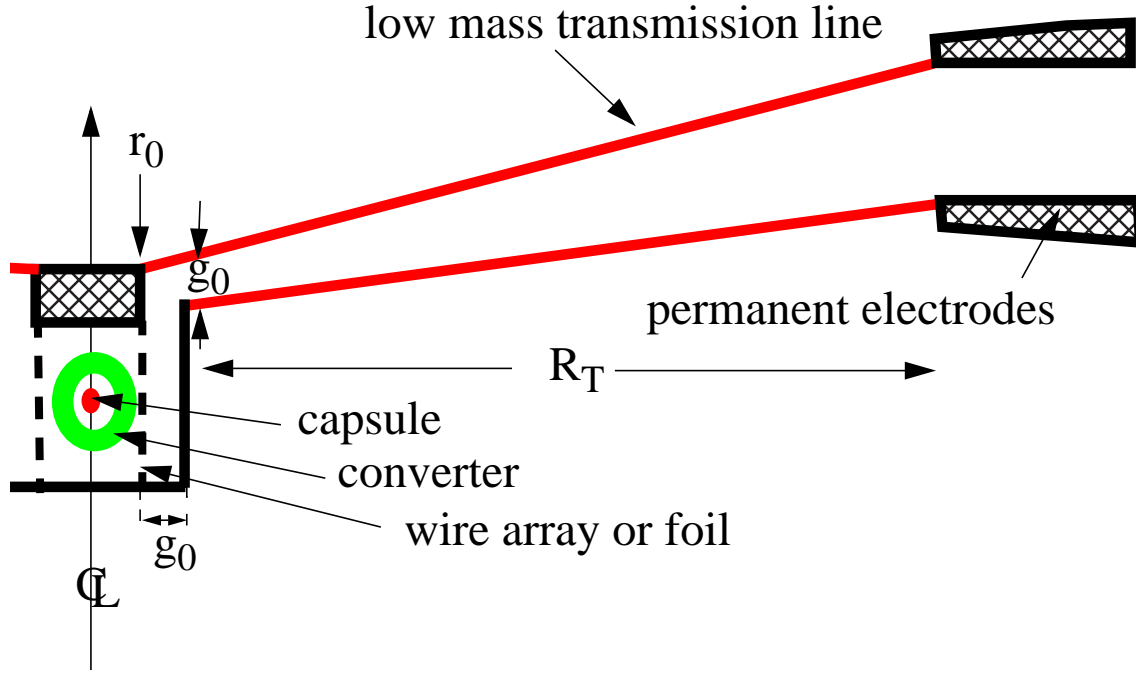


Fig. 1 A schematic of a Low Mass Transmission Line

Power flow experiments indicate that the gap must remain finite near the pinch. Therefore we assume a gap given by

$$g = g_0 + \Delta\theta(r - r_0). \quad (4)$$

Using Eqs. (3) and (4) we can solve for the areal density of the electrodes

$$\Gamma(r) = \frac{11\sqrt{3}(\mu_0)}{112\pi(4\pi)} \frac{t_p^2 I_p^2}{\Delta g r^2 [g_0 + \Delta\theta(r - r_0)]} \quad (5)$$

which scales roughly as r^{-3} for $r \gg r_0$. At some radius, r_x , the areal density of the electrode as calculated by Eq. (5) could be smaller than a minimum, Γ_n , required for structural strength or to conduct the current with acceptable resistive losses. We shall assume that $\Gamma = \Gamma_n$ for $r > r_x$. The total transmission line mass is then found from the integral.

$$M_{TOT} = 2 \int_{r_0}^{R_T} 2\pi r \Gamma(r) dr \quad (6)$$

with the result

$$M_{\text{TOT}} = \frac{11\sqrt{3}}{28\Delta g} \left(\frac{\mu_0}{4\pi} \right) \frac{t_p^2 I_p^2}{[g_0 - \Delta\theta r_0]} \ln \left\{ \frac{g_0 r_x}{r_0 [g_0 + \Delta\theta (r - r_0)]} \right\} + 2\pi \Gamma_n (R_T^2 - r_x^2). \quad (7)$$

Since this function decreases monotonically with $\Delta\theta$, it is instructive to consider the limit $\Delta\theta = \Gamma_n = 0$, which yields

$$M_{\text{TOT}} = \frac{11\sqrt{3}}{28\Delta g} \left(\frac{\mu_0}{4\pi} \right) \frac{t_p^2 I_p^2}{g_0} \ln \left(\frac{R_T}{r_0} \right). \quad (8)$$

Using values appropriate for a fusion reactor, i.e. $I_p = 100$ MA, $r_0 = 3$ cm, $R_T = 4$ m, $t_p = 150$ ns, and $\Delta g = 0.1$, we obtain the surprisingly small result that $M_{\text{TOT}} = 0.37$ kg. This should be compared to the mass of the transmission line in the Z accelerator, which weighs approximately 5 tons. Using these same parameters, eq. (5) yields

$$\Gamma(r) = \frac{11\sqrt{3}}{112\pi} \left(\frac{\mu_0}{4\pi} \right) \frac{t_p^2 I_p^2}{\Delta g r^2 g_0} = \frac{6.1 \times 10^{-3}}{r^2} \text{ kg/m}^2, \quad (9)$$

where r is in meters. At a 1 meter radius, this corresponds to an electrode thickness of 0.75μ for steel or 6μ for plastic. If such extremely thin electrodes can not be constructed which can carry the large currents needed to drive the z pinch, the mass of the transmission line will be dominated by the second term in eq. (7) and to a good approximation the transmission line mass needed to drive a fusion capsule is given by the simple expression

$$M_{\text{TOT}} = 2\pi \Gamma_n R_T^2. \quad (10)$$

In the next section we present the results of experiments on the Saturn facility to determine the appropriate value of Γ_n .

III. Low Mass Transmission Line experiments

In the last section it was found that, at the outer portion of the LMTL, very thin electrodes have sufficient inertia to resist the current generated magnetic pressure. This electrode thickness is much smaller than the resistive skin depth of typical cold electrode materials ($\sim 50 \mu$ for aluminum). This suggests that there might be excessive resistive losses if very thin electrodes are used. However, it is difficult to calculate the magnitude of this effect, due to the complicated nature of surface breakdown phenomenon, which can lead to highly conducting plasmas. Therefore we designed an experiment to investigate the resistive effects of very thin electrodes. A schematic of the experimental set up is depicted in Fig. 2. A diagram of the actual hardware is shown in Fig. 3. Current is fed from the top by the Saturn accelerator with a nominal maximum short circuit current of about 10 MA. The test hardware is a coaxial transmission line with a short circuit at the end furthest from the accelerator (bottom). Since the transmission line is only 30 cm long it acts as a lumped inductance of approximately 4 nH. This brings the peak expected current down to about 9 MA. The hardware is divided into three azimuthal sections of 120 degrees each, which are held together on the top and bottom by rings. Current monitors (Bdots) are placed in each of the azimuthal segments at the positions labelled in Fig. 2. The top and bottom Bdots determine the degree of magnetic insulation obtained within the transmission line. The top and bottom Bdots should have the same current profiles if the transmission line is 100% insulated. If the test electrode has a significant resistance, current will flow through the shunt electrode. This current is monitored by the middle Bdots.

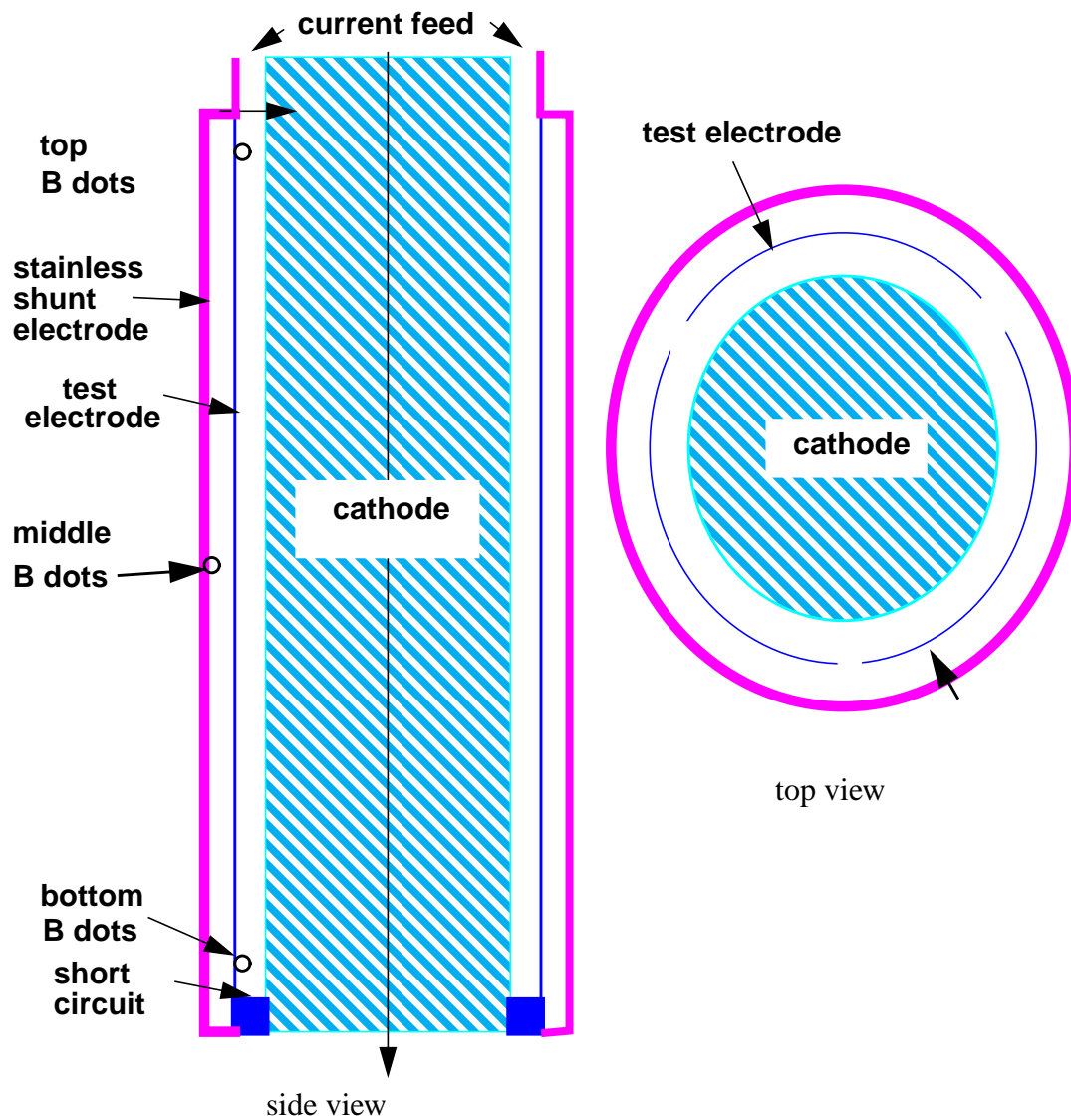


Fig. 2 A schematic of the experimental design

Three carbon steel test electrodes of thicknesses 50, 100, and 250 μ were tried. Carbon steel has been identified as an excellent electrode material for z pinch driven fusion energy, due to its low activation and good separability from the reactor coolant material fiibe. We also tried a 20 μ of mylar test electrode as a possible candidate material for pulsed nuclear space propulsion.

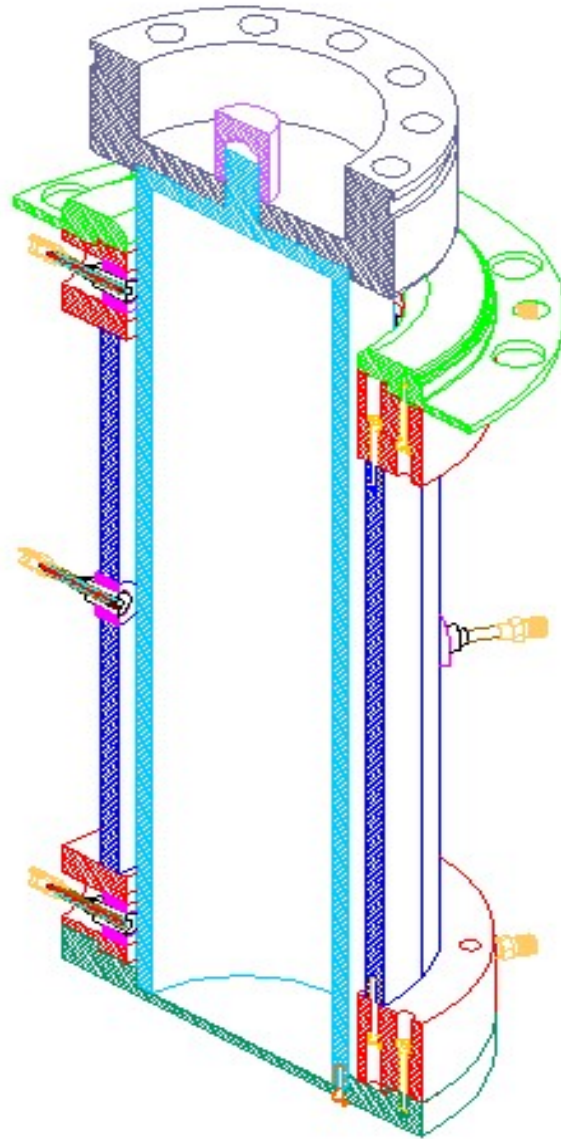


Fig. 3 The experimental set up 3D cutaway

The first shot (Saturn shot2962) used a $100\ \mu$ carbon steel test electrode. The measured currents are plotted in Fig. 4. The current measured at the bottom is slightly higher than at the top for a period of time. Since this is not actually possible, the difference gives some measure of the accuracy of the measurements. The current measured by the middle Bdots, is considerably lower than either the top or the bottom for the first 100 ns of the pulse. Thus most of the current is being carried by the test electrode during the time of a typical z

pinch implosion (~ 1.2 to 1.3 time the current risetime). The top and bottom current monitors remain near the peak current for 400 ns after the initial rise. This is a behavior that has often been seen with Bdot monitors. It is often assumed that the Bdots “flash” (short out possibly due to plasma formation in the loop) and do not register the negative voltage required to bring the integrated current back down. However, the rising current measured by the middle Bdots in this experiment imply that there is at least 4 MA of current carried by the cathode 400 ns after the initial current rise. This suggests that the top and bottom Bdots may not have flashed and are actually measuring current which takes a long time to be resistively damped.

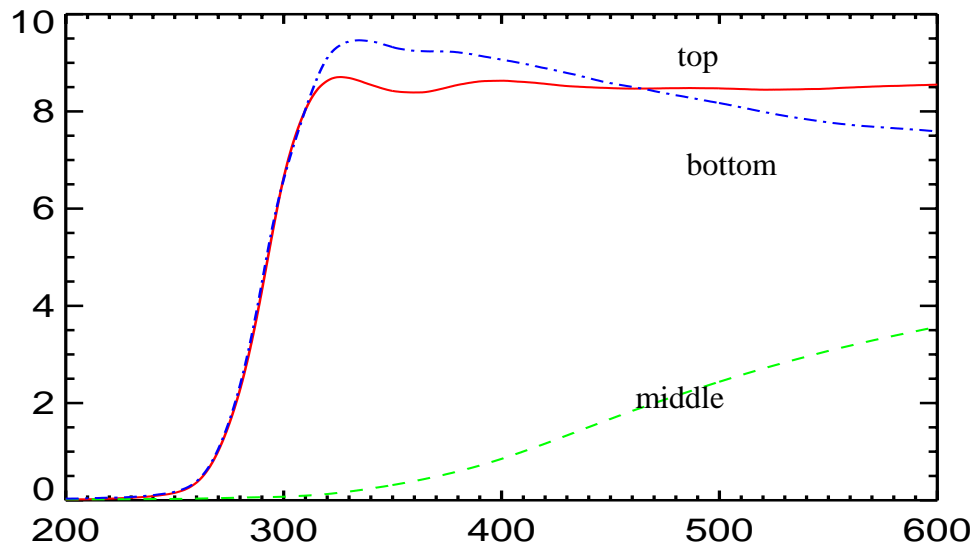


Fig. 4 The currents plotted as a function of time for shot 2962 (100 μ carbon steel)

This data can be used to obtain an effective resistance of the test electrode. The current carried by the test electrode is the difference between the bottom and the middle currents. The voltage across the test electrode is approximately LdI/dt where $L \sim 4$ nH is the inductance between the test and shunt electrodes (gap = 3 mm) and dI/dt is given by the uninte-

grated middle Bdots. Dividing the voltage across the test electrode by the current it carries yields a measure the resistance of the test electrode. This is plotted in Fig. 5

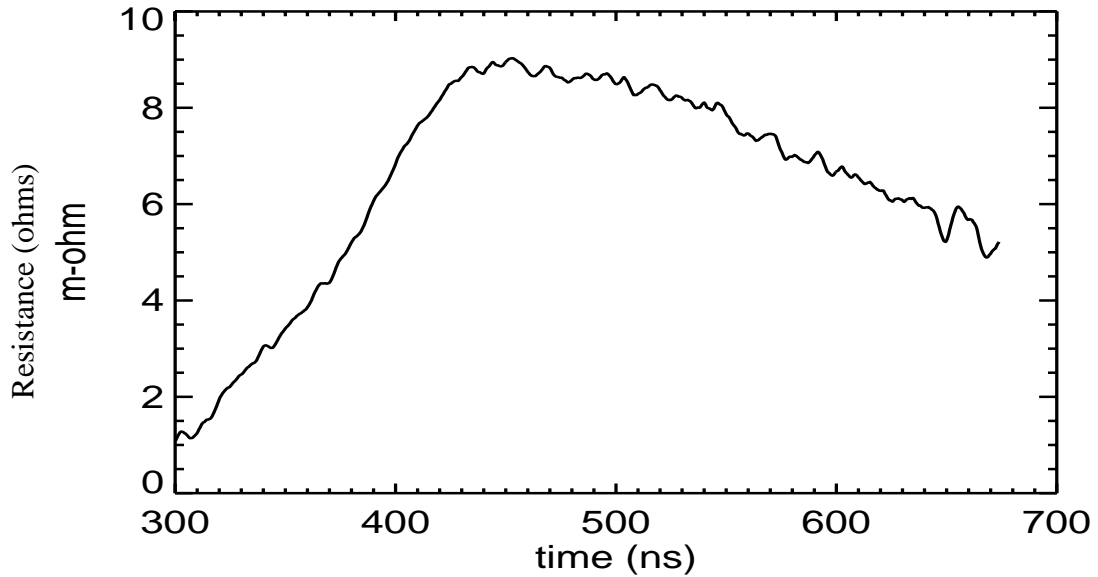


Fig. 5 The effective resistance across the test electrode is plotted as a function of time for shot 2962

The rising portion of the resistance is probably due to the finite time it takes for the magnetic field to diffuse through the test electrode. The falling portion of the curve should be more representative of the true resistance of the electrode. We estimate the energy lost due to joule heating given by the integral $E_{\text{joule}} = \int_0^t R(t)I(t)^2 dt$ where $I(t)$ is the full current entering from the test LMTL. This is plotted in Fig. 6. An optimal z-pinch implosion occurs a little after peak current (~ 350 ns) in this experiment. At that time the resistive loss is approximately 10 kJ. This is less than 10% of what Saturn could deliver to a z-pinch load (~ 140 kJ). The z-pinch energy and the resistive loss both scale as I^2 , but the resistive loss also scales as L_T/r_T , where L_T is the length of the transmission line and r_T is the radius. If we scale our experimental data up to a transmission line carrying 100 MA of current we must increase the transmission line radius by roughly a factor of 10 ($r_T = 40$ cm) to maintain the same current density. Increasing the transmission line length by the same factor ($L_T = 3$ m) will hold the resistive losses to 10% of the z-pinch energy.

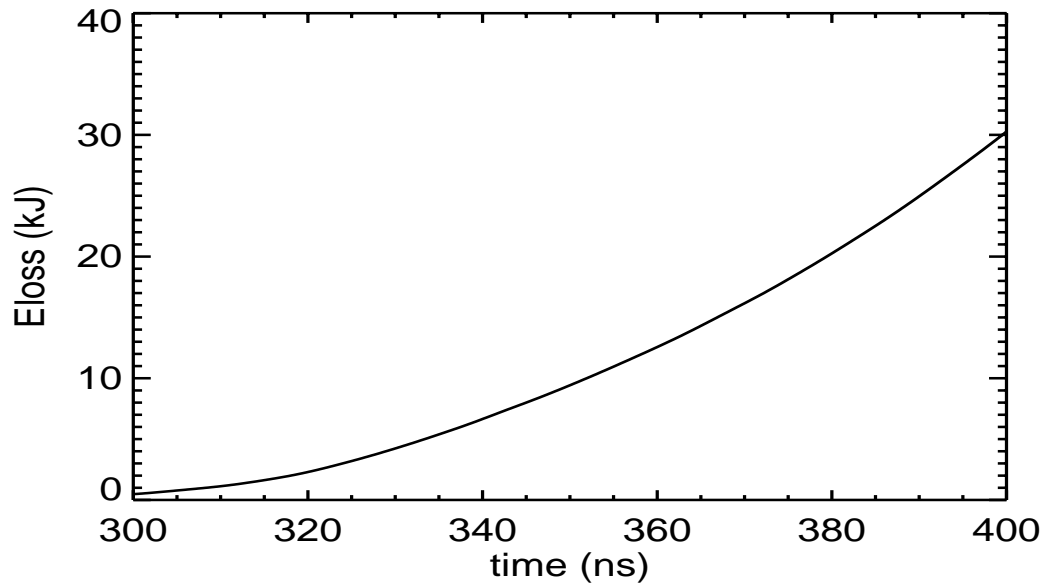


Fig. 6 The resistive loss in the test electrode is plotted as a function of time for shot 2962

Our second shot (Saturn shot 2963) used a 20 μ mylar test electrode. The currents are plotted in Fig. 7.

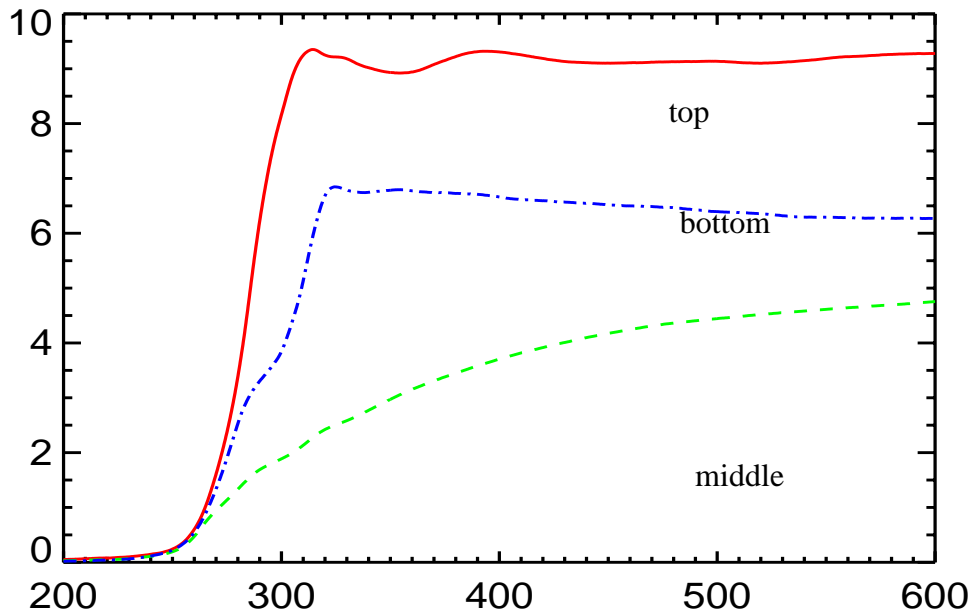


Fig. 7 The currents plotted as a function of time for shot 2963 (20 μ of mylar)

There is a significant difference between the top and bottom currents indicating a substantial loss of magnetic insulation. The hardware showed evidence of this loss near the top connection of the test electrode. This connection was made with epoxy, which may be responsible for the loss. However, even with this loss, approximately 7 MA of current was delivered through the mylar test electrode. The resistance calculated in the same manner as the previous shot is shown in Fig. 8

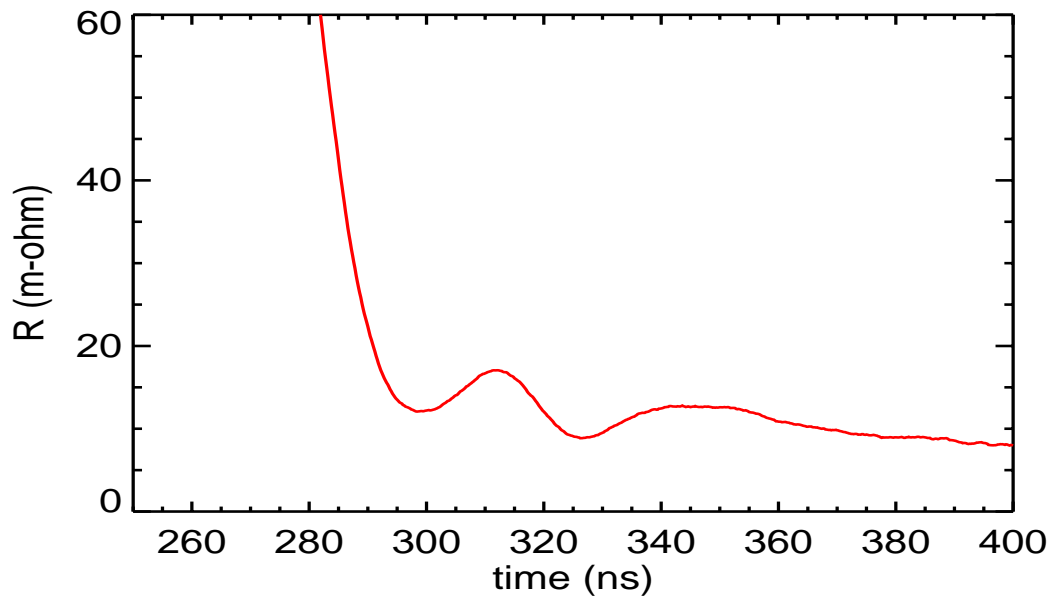


Fig. 8 The resistance of the 20 μ mylar test electrode plotted as a function of time

The initially high resistance may be because mylar is an insulator before electrical breakdown. The energy lost due to resistivity $\int I^2 R dt$ is plotted in Fig. 9

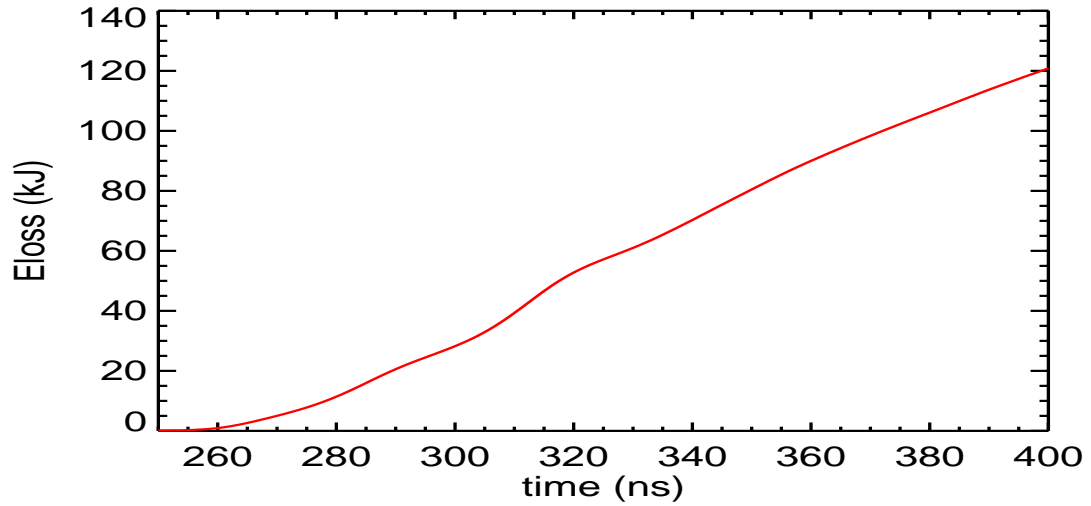


Fig. 9 The resistive loss in the test electrode is plotted as a function of time for shot 2963 with a 20 μ mylar test electrode

The resistive losses at 350 ns are approximately 75 kJ, which is about 54% of the energy that would be available to a z pinch. This result scales to a 3 m long transmission line carrying 100 MA of current. Although this is a significant loss, it may still be acceptable for propulsion applications where transmission line mass is extremely important.

A 50 μ thick test electrode of carbon steel was tested on shot 2964. The currents are shown in Fig. 10

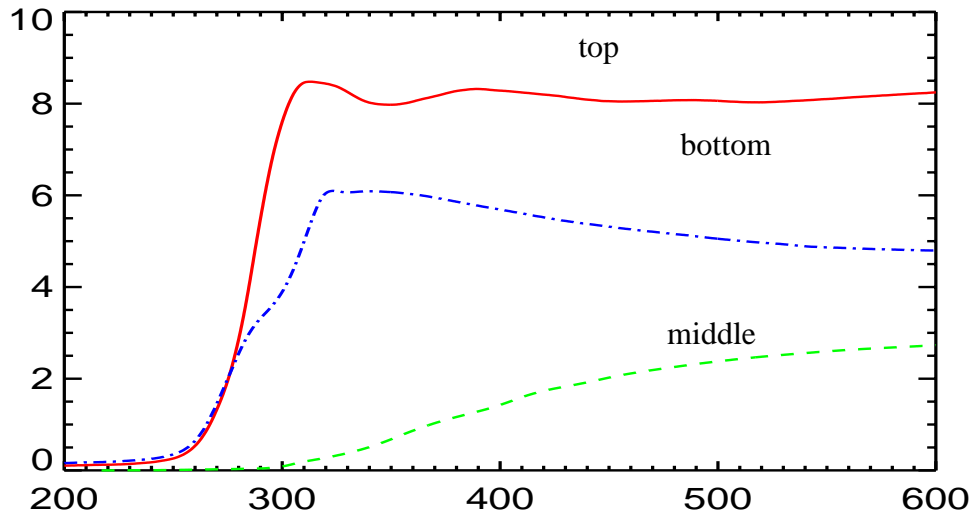


Fig. 10 The currents plotted as a function of time for shot 2964, with test a 50 μ thick carbon steel electrode

This shot showed some loss of magnetic insulation evident by the difference between the top and bottom signals. The hardware was damaged at the upper connection point of the test electrode as in the previous shot. However, about 6 MA of current was delivered the full length of the transmission line and we can calculate the effective resistance from this data. The result is plotted in Fig. 11. As one would expect, the result is intermediate between the thin mylar and the 100 μ carbon steel shot. The resistive energy lost in the test electrode is plotted in Fig. 12. Approximately 40 kJ is lost by 350 ns (approximate pinch collapse time). This is about 28% of the energy that could be delivered to a pinch.

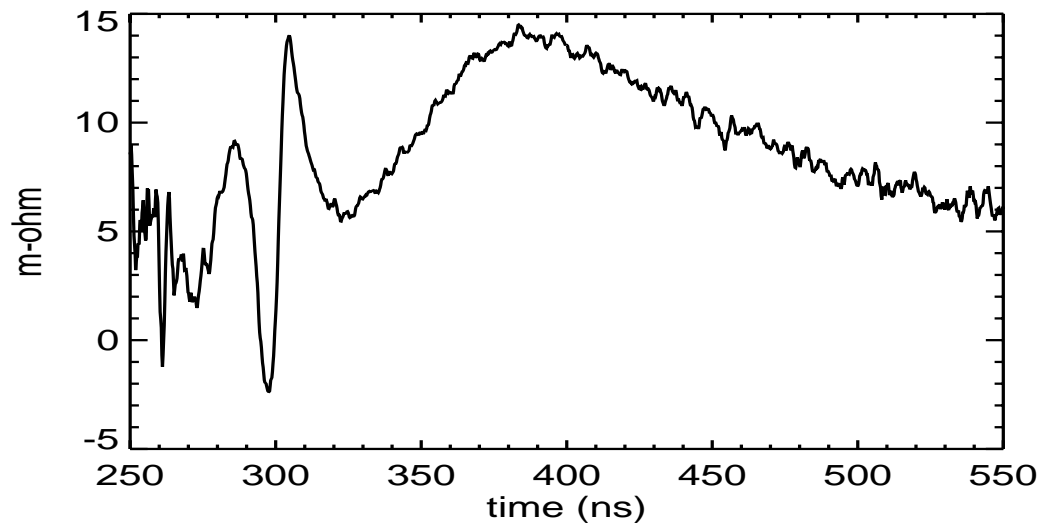


Fig. 11 The effective resistance as a function of time for a 50 μ thick test electrode (shot 2964)

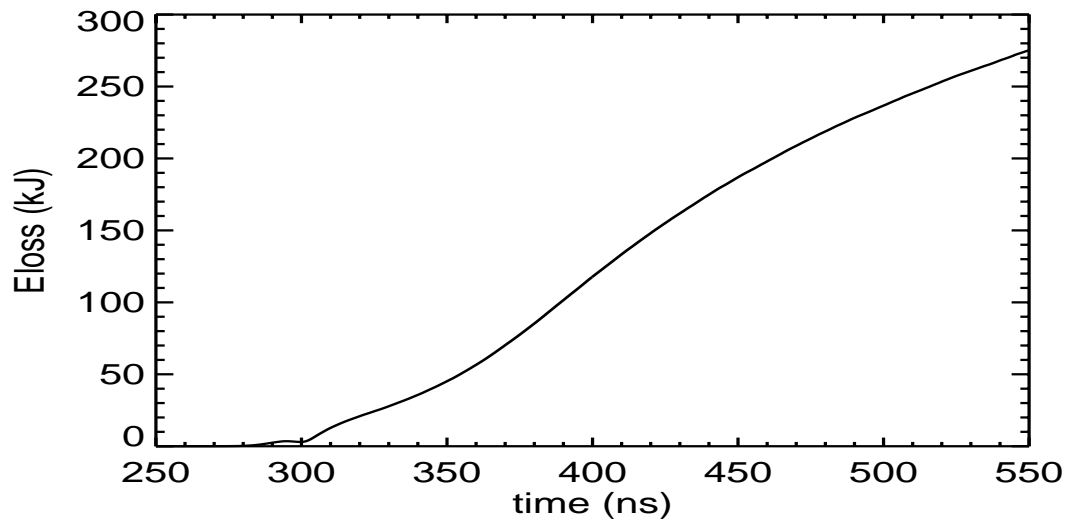


Fig. 12 The resistive energy loss as a function of time for a 50 μ thick test electrode (shot 2964)

The last shot (2965) test a 250 μ thick carbon steel electrode. The current waveforms are shown in Fig. 13. As can be seen, there is significant loss of current between the top and bottom. The hardware showed damage near the top connection of the test electrode.

Approximately 5 MA of current reached the bottom. The middle current is very small, which indicates that the test electrode carried nearly all of the current.

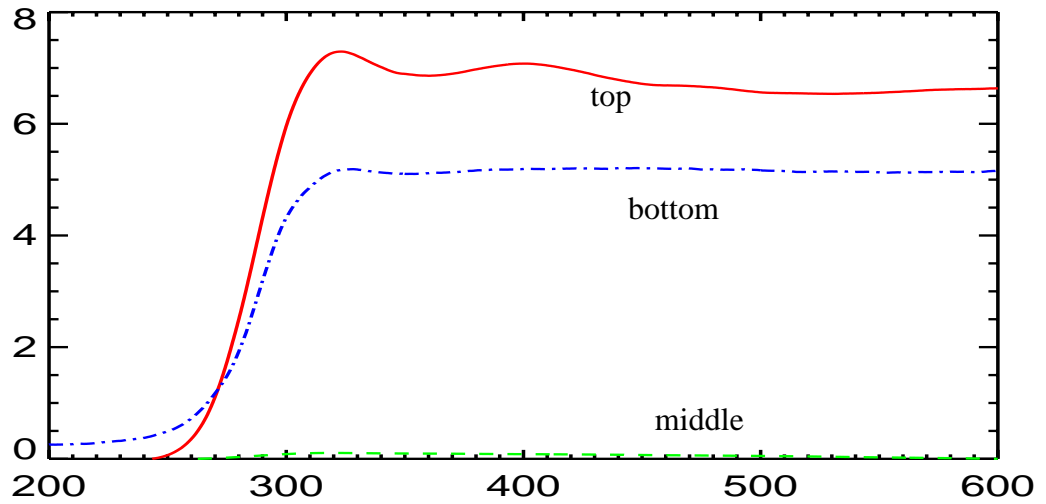


Fig. 13 The current waveforms are plotted as a function of time for a 250 m thick carbon steel test electrode (shot 2965)

The resistance is plotted as a function of time Fig. 14

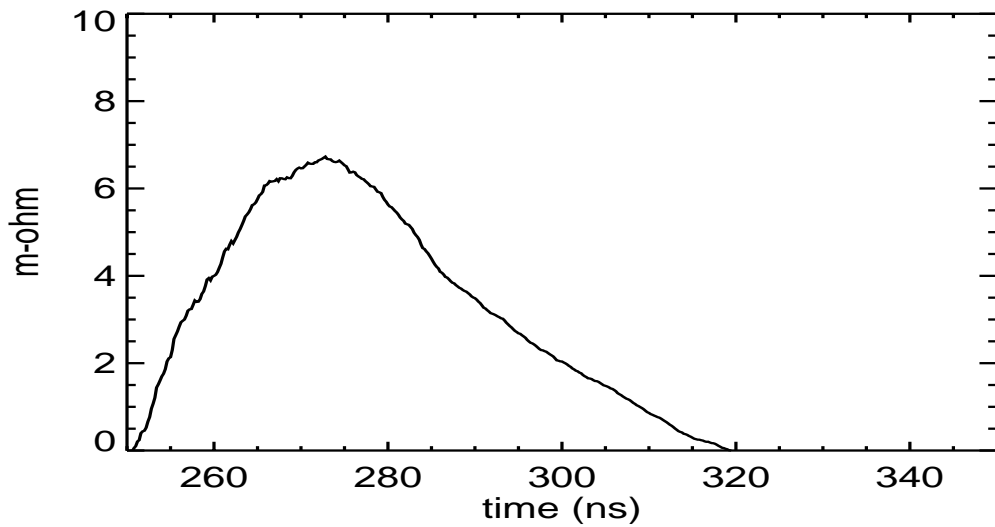


Fig. 14 The effective resistance is plotted as a function of time for a 250 m thick carbon steel test electrode (shot 2965).

The resistive energy loss is plotted in Fig. 15

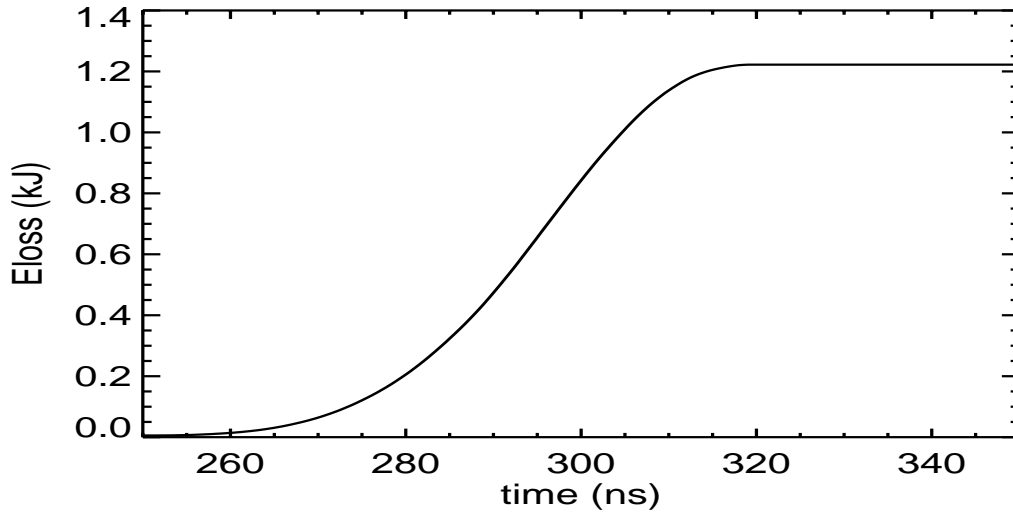


Fig. 15 The resistive energy loss is plotted as a function of time for a 250 m thick carbon steel test electrode (shot 2965).

The resistive energy lost at 350 ns is less than 1% of the energy that could be delivered to a z pinch. Clearly, increasing the electrode thickness will have a negligible effect on the power flow.

We normalize the current carried by the shunt electrode to the peak of the bottom current. This fraction is plotted as a function of time for all the shots in Fig. 16. As can be seen the fraction is smaller for the thicker electrodes. Note that in a reactor geometry the only shunt path would be the reactor walls. This path would be highly inductive and so nearly all of the current would have to flow in the transmission line electrode even if it was very thin. The losses would then be limited to resistive losses. We have estimated the resistive losses for each shot. We divided this by the energy available to drive a z pinch (~140 kJ) to obtain a fractional resistive loss for each shot. The results are plotted in Fig. 16.

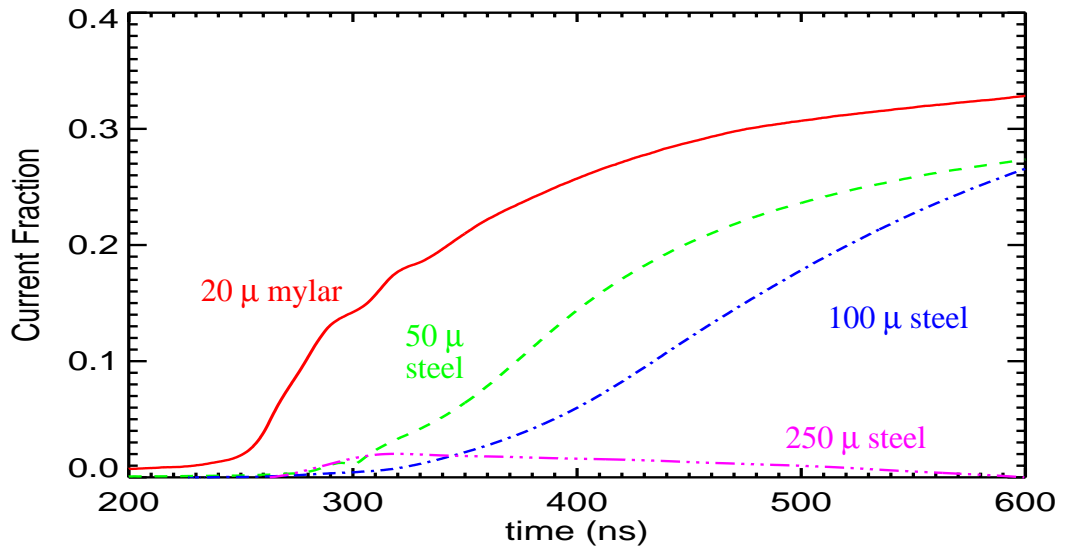


Fig. 16 The fraction of the current carried by the shunt electrode as a function of time for each of the shots.

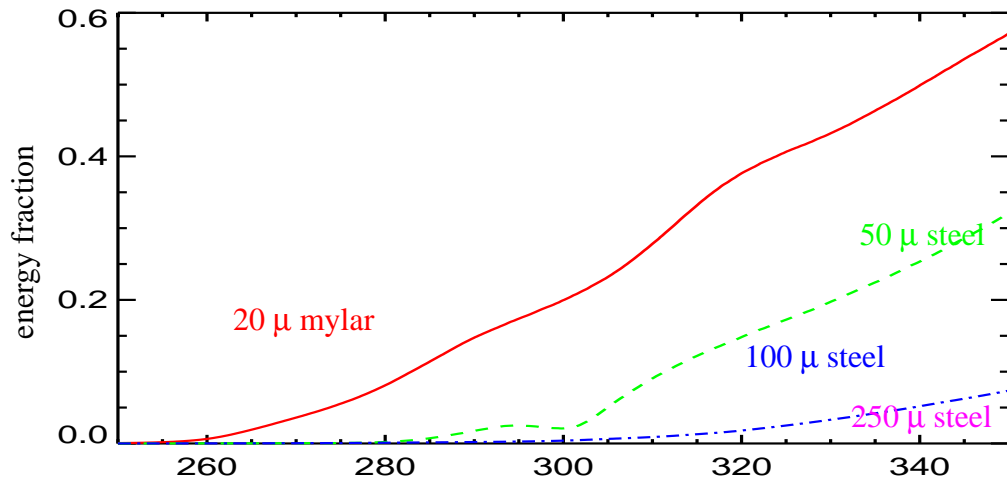


Fig. 17 Calculated fraction of the available energy lost to resistance of the test electrodes as a function of time.

The progression of smaller losses as the electrode thickness is increased is clearly indicated. The losses from the 20 μ mylar at 350 ns could be considered acceptable. The losses from 50 μ of steel are almost certainly acceptable. Increasing the thickness to 100 μ

or more reduces the losses to an insignificant fraction of the energy that could be delivered to a z pinch.

We use eq. (10) to estimate the total mass for a reactor scale LMTL ($R_T = 4$ m) assuming the minimum areal density is the same as each of the test electrodes. The results are summarized in table 1

Table 1:

electrode	Γ (kg/m ²)	M_{TOT} (kg)	Efficiency%
20 μ mylar	0.02	2.0	45
50 μ steel	0.4	40.0	70
100 μ steel	0.8	80.0	90
250 μ steel	2.0	200.0	98

With the exception of the 20 μ mylar case, these masses are large compared to the result of eq. (8) and we are justified in using eq. (10). These results indicate that the LMTL mass can be quite modest (~80 kg) with a very small resistive loss (<10%). Such low masses should reduce the cost of recycling transmission lines in an ICF fusion energy application. However, eq. (10) is not an adequate approximation for applications such as microfission or magnetized target fusion that use long current pulses (> 150 ns). We then need to determine the appropriate value of $\Delta\theta$, which is determined by requirements of power flow in the transmission line.

IV. Power flow

A. Magnetic insulation

We shall now find the relationship between the value of $\Delta\theta$ and the degree of self-magnetic insulation of the LMTL. The condition for magnetic insulation is approximately

$$V < Bgc, \quad (11)$$

where V is the voltage applied to the transmission line. The time for the current pulse to propagate through the transmission line will be short ($\sim R_T/c \sim 10$ ns) relative to the risetime of the pulse (> 100 ns) and so it will act approximately as a lumped inductance. The voltage along the transmission line will then be given by the expression

$$V(r) = L_{TL}(r) \frac{dI}{dt} + \frac{d}{dt}(L_p I) \quad (12)$$

where L_p is the inductance of the z pinch and $L_{TL}(r)$ is the inductance of the transmission line between the pinch and a radius, r . The inductance of the z pinch increases as the pinch collapses. The radius of the pinch can be calculated analytically for the current profile of Eq. (2) with the result $r = r_0(1 - \tau^4)$. The pinch inductance is thus

$$L_p \leq \frac{\mu_0}{2\pi} l_p \ln\left(\frac{r_0 + g_0}{r_0(1 - \tau^4)}\right) \quad (13)$$

where g_0 is the initial gap between the pinch and the return current electrode, r_0 is the initial radius of the pinch plasma and l_p is the length of the pinch. We place an upper limit on the pinch inductance during the rising portion of the current pulse by using the pinch radius at peak current, i.e. $r = 2r_0/3$. Using $g_0 = 2$ mm, $r_0 = 3$ cm and $l_p = 2$ cm we find that $L_p \sim 2$ nH.

The inductance of the transmission line is

$$L_{TL}(r) = \frac{\mu_0}{2\pi} \left\{ (g_0 - \Delta\theta r_0) \ln\left(\left(\frac{r}{r_0}\right) + \Delta\theta(r - r_0)\right) \right\}. \quad (14)$$

Substituting Eqs (13)-(14) into Eqs. (12) and Eq. (11), then setting $\frac{dI}{dt} = \frac{I_p}{t_r}$, and using the maximum value of L_p , we find that $\Delta\theta \geq \theta_{\min}$ where

$$\theta_{\min} = \max \left(\frac{g_0 \left(\ln \left(\frac{r}{r_0} \right) - \frac{F_L c t_r}{r} \right) + \frac{2\pi L_p}{\mu_0}}{\left(R_T - r_0 \right) \left(\frac{F_L c t_r}{r} - 1 \right) + r_0 \ln \left(\frac{r}{r_0} \right)} \right), \quad (15)$$

for $r \in [r_0, R_T]$, where F_L is the fraction of the peak current needed before the transmission line is magnetically insulated, and t_r is the time to peak current. Defining

$$\alpha = \frac{F_L c t_r}{R_T}, \quad (16)$$

we find

$$\theta_{\min} = \frac{g_0 \left(\ln \left(\frac{R_T}{r_0} \right) - \alpha \right) + \frac{2\pi L_p}{\mu_0}}{\left(R_T - r_0 \right) (\alpha - 1) + r_0 \ln \left(\frac{R_T}{r_0} \right)}. \quad (17)$$

Setting $R_T = 4$ m, $r_0 = 3$ cm, and $L_p = 3$ nH, the minimum angle is plotted as a function of α in Fig. 18

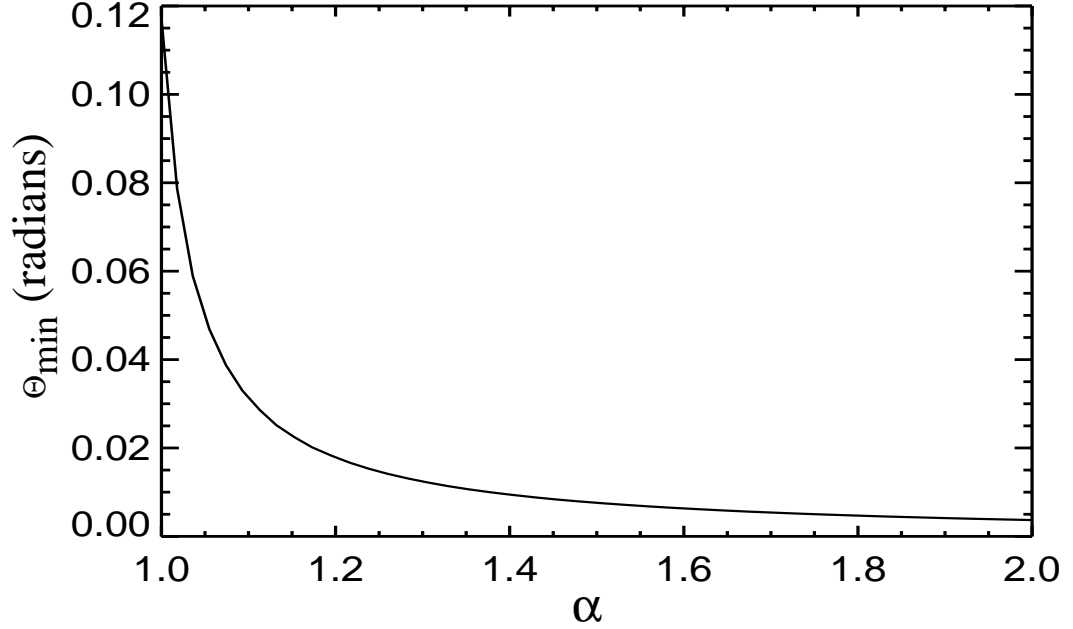


Fig. 18 The calculated minimum angle between the transmission line electrodes is plotted as a function of α .

As can be seen, the minimum angle decreases strongly with increasing α . Substituting this result into eq. (7), we calculate the transmission line mass which is plotted in Fig. 19 as a function of α . The parameters of the calculation were chosen to be consistent with a high yield capsule suitable for energy. The parameters are, $\Delta g = 0.1$, $I_p = 100$ MA, $\Gamma_n = 0.02$ kg/m². The mass increases for small angles because the gap between the electrodes is smaller and less electrode motion can be tolerated to maintain the same Δg .

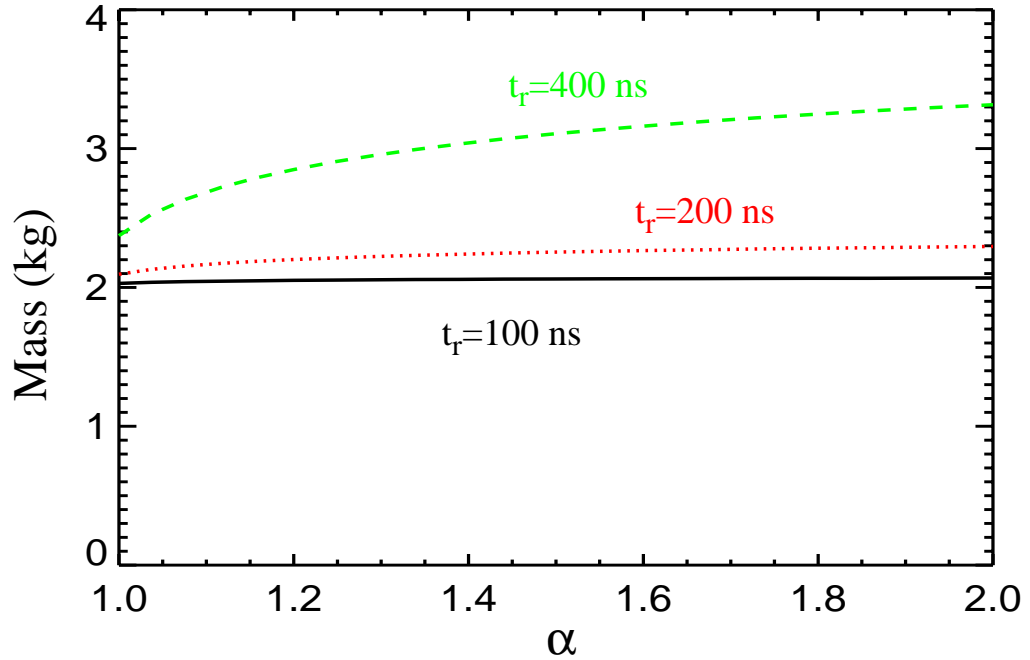


Fig. 19 The LMTL mass plotted as a function of α for several values of the current risetime.

The smallest value of t_r corresponds to the present Z machine and the mass is nearly independent of α because the second term in eq. (7) dominates. As can be seen the first term of eq. (7) cannot be ignored as t_r is increased. Clearly the transmission line mass is minimized by decreasing α . Note that α must be greater than zero to maintain a finite value of θ_{\min} . However, increasing $\Delta\theta$ increases the transmission line inductance and thus the voltage needed to drive the current. Using eqs. (12) and (14), the driving voltage has been

calculated. The results are shown in Fig. 20. As can be seen, the voltage is decreased by increasing the rise time of the current pulse.

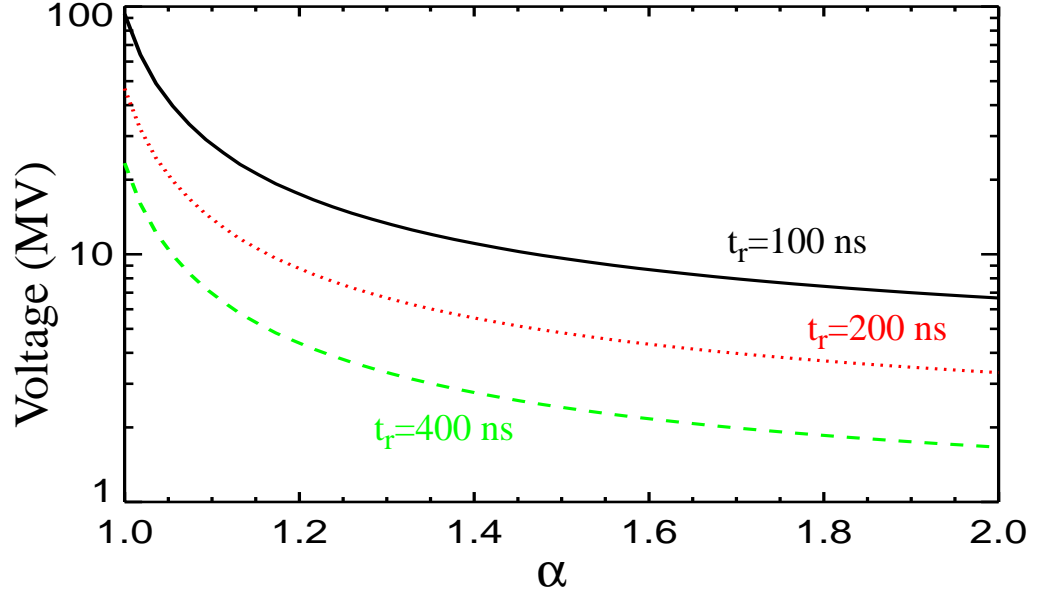


Fig. 20 The required driving voltage is plotted as a function of α for several values of the current risetime.

Since the power is the product of current times voltage, it is clear that the total energy delivered to the transmission line will increase with driving voltage. However, the energy delivered to the pinch is only dependent on the current as given by the formula²

$$E_p = \sqrt{3} I_p \left(\frac{\mu_0}{2\pi} \right) I_x^2. \quad (18)$$

Thus the efficiency of delivering energy to the pinch will increase with α . We calculate this efficiency using Eqs. (2) and (11)-(18). The result is plotted in Fig. 21 for two values of the transmission line radius. As can be seen, the efficiency is not a strong function of the transmission line radius. Note that it is independent of the current risetime at a fixed value of α .

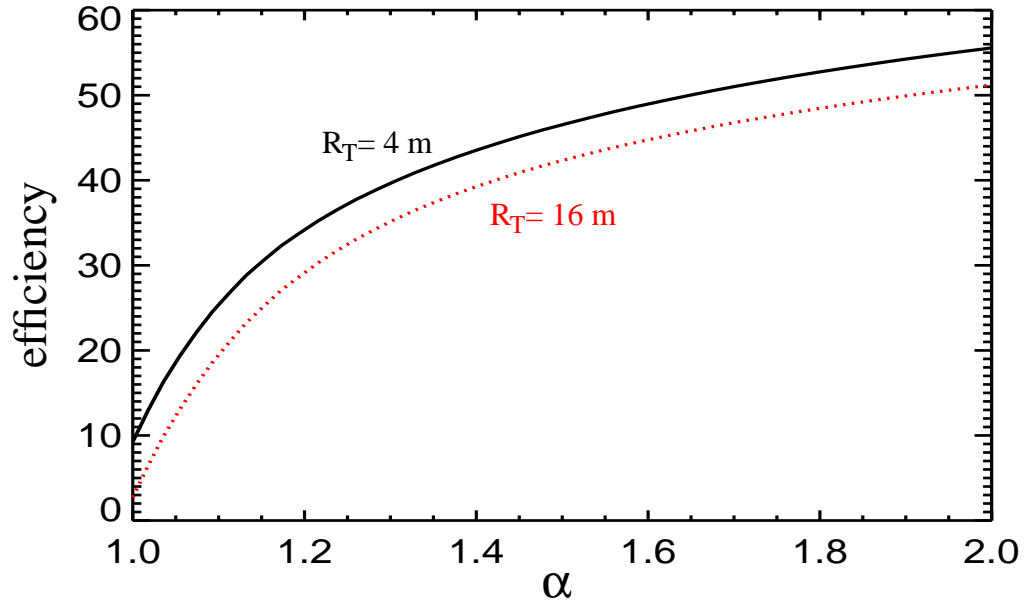


Fig. 21 The efficiency is plotted as a function of α for two values of the transmission line outer radius

Equation (16) indicates that increasing α corresponds to greater current lost before the transmission line becomes self magnetically insulated. If the transmission line remains uninsulated for too long, surface plasmas may be formed. These plasmas could cause unacceptable leakage current later in the pulse. Therefore there is a maximum practical value for α . The existing Z accelerator is self insulated at about 0.15 of the peak current, i.e. $F_L=0.15$. This corresponds to $\alpha \sim 1.5$ for a 150 ns risetime. Experiments will be needed to determine if larger values of α can be used and if the value depends on the risetime of the current pulse. Using the value $a = 1.5$ the transmission line mass is only 2 kg for a 150 ns risetime current pulse. Such a low mass make recycling much easier for energy applications.

B. Ion losses

The results of our experiments indicate that $\Gamma_n \sim 0.02 \text{ kg/m}^2$. This corresponds to a 20 micron mylar foil, which is fairly strong, but would wrinkle easily. These wrinkles could

be smoothed out by applying outward tension at the transition between the permanent electrodes and the LMTL. There may be some difficulty removing all of the wrinkles if the electrodes are a complete disk. A convenient alternative is to use triangular shaped ribbons as shown in Fig. 22. This arrangement should make it much easier to remove wrinkles, but the edges could enhance a plasma breakdown process. This could be a concern if such a plasma forms on the anode side of the transmission line and allows ions to be accelerated across the gap. This ion current would not be delivered to the z pinch and thus is a loss.

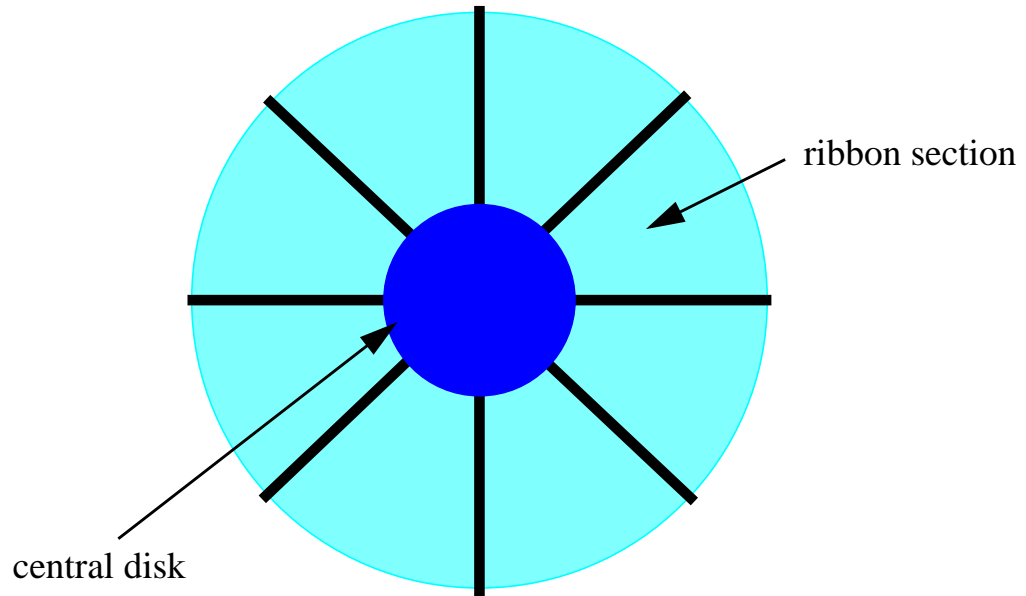


Fig. 22 A schematic of a disk electrode composed of triangular ribbon sections

The magnitude of this effect can be estimated as follows. Assume that some fraction, f_a , of the available anode area forms a plasma that acts as a space-charge-limit ion source. The ion current density is then given by the Child-Langmuir law

$$J = \frac{4}{9} \epsilon_0 \sqrt{\frac{2e}{m}} \frac{V^{3/2}}{d^2} \quad (19)$$

If we assume $d = \Delta\theta$ the voltage found from Eq. (12), is simplified to the following form

$$V \approx \frac{\mu_0}{2\pi} \Delta\theta \frac{I_p}{t_r} r. \quad (20)$$

We then perform the integral

$$I_{\text{loss}} = \int_0^{R_T} 2\pi J r dr \quad (21)$$

with the result

$$\frac{I_{\text{loss}}}{I_p} = \frac{8}{27} \left(\frac{e\mu_0 I_p}{\pi m \Delta\theta} \right)^{1/2} f_A \frac{R_T^{3/2}}{c^2 t_r^{3/2}} \approx 0.26 f_A \quad (22)$$

assuming $I_p = 100$ MA, $L_s = 4$ meters, and $\Delta\theta = 0.01$ which corresponds to $a = 1.5$, see Fig. 18. Since plasma will only be formed at the boundaries, $f_A \ll 1$ and the ion loss current should be negligible. This analysis suggests that ribbons could be used. In fact the experiments reported in section III used three sections.

V. Pulsed Nuclear Space Propulsion

The Orion concept was based on numerous rather large fission explosions. Consequently the space craft was also very large. An alternative is to use microfusion or microfission explosions to reduce the size of the craft. A schematic of a pulsed nuclear rocket based on pulsed power driven micro explosions is shown in Fig. 23. Current generated from a pulsed power network is delivered through a section of permanent transmission line and then through a section of LMTL (which will be destroyed each shot.) to the micro explosive unit. The explosive unit could be either an inertial fusion capsule or a microfission device. Large currents will be required in either case (60-100 MA). The primary different will be the optimum current risetime. This is about 150 ns for a z-pinch driven fusion microexplosion, while the optimum current risetime to drive microfission could be as long as 10 μ s.

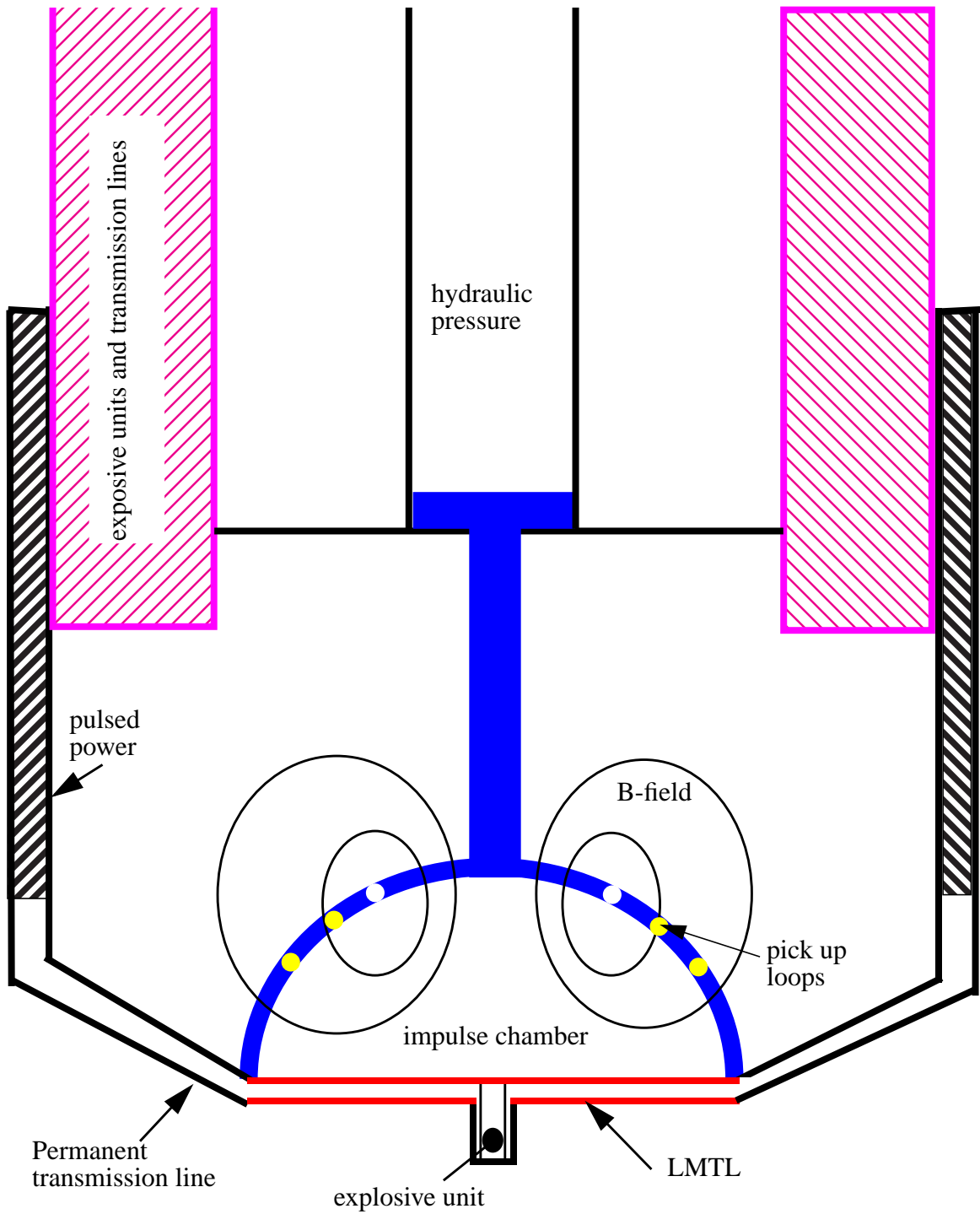


Fig. 23 A schematic of a nuclear rocket driven by pulsed power

The yield from the microexplosion needs to be large enough to vaporize the LMTL. The plasma generated from the LMTL material and the explosive unit will be expand at high velocity. The characteristic velocity of this expansion is given

$$v_c = \sqrt{\frac{2Y}{M_{TOT}}} \quad (23)$$

where M_{TOT} is the total mass of the explosive device and the transmission line. The portion of this mass that expands toward the impulse chamber will stagnate against the magnetic field and be redirected downward to participate as expelled rocket propellant. The average exhaust velocity of the rocket propellant will be some fraction of the characteristic exhaust velocity, i.e.

$$v_{ex} = gI_{sp} \approx \eta \sqrt{\frac{2Y}{M_{TOT}}}, \quad (24)$$

where, I_{sp} is the specific impulse, and η is a factor less than one which accounts for non-ideal effects such as plasma velocity components at an angle to the rearward direction and the nonuniform heating of the transmission line. An estimate of the effects of nonuniform heating is given in the appendix. The result indicates a value of $\eta \approx 0.5$

An optimum trade-off between propellant mass and power requirements occurs when the exhaust velocity approximately matches the final space craft velocity. As an example a ΔV of 30 km/s would allow a round trip to Mars in approximately 150 days. The yield required to obtain this exhaust velocity is $Y = 1.8M_{TOT}$ GJ where M_{TOT} is the mass in kg. This clearly demonstrates that LMTLs are critical to nuclear pulsed rockets using micro explosions. Although yields in excess of 1 GJ, will be required, these are still micro explosions when compared the explosions considered for the Orion³ space vehicle which were about 20,000 GJ.

We shall now estimate of the required standoff distance between the microexplosion and permanent components of the rocket. This standoff distance will be the outer radius of the LMTL and will be needed to calculate the LMTL mass using Eq. (7). The pressure generated by the explosion is approximately $P_X = \frac{3Y}{4\pi r^3}$. Although the impulse chamber is a hemisphere, the stress on the open end will be similar to that which would be exerted on a tube and thus the stress is $\sigma = P_x \frac{r}{\Delta r}$, where Δr is the wall thickness. The maximum tensile strength of steel is about 5×10^9 nt/m². We shall design with a maximum stress of $\sigma_T = 1.25 \times 10^9$ to introduce a generous safety margin. From these considerations we find that the mass of the impulse chamber is $M_{IC} = \frac{\rho_s Y}{\sigma_T} \sim 3.2 \times 10^3$ kg for a 1 GJ yield, where $\rho_s \approx 8000$ kg/m³ is the density of steel. The standoff is then

$$r_T > \left(\frac{3Y}{4\pi\sigma_T} \frac{r}{\Delta r} \right)^{1/3} \sim 1.2 Y_{GJ}^{1/3} \text{ meters}, \quad (25)$$

for $r/\Delta r=10$. Note that increasing the ratio $r/\Delta r$ to 100 only doubles the required standoff.

The total impulse delivered to the chamber will be $I_{IC} = \eta \sqrt{2YM_{TOT}}$. The velocity of the chamber just after the explosion will then be I_{IC}/M_{IC} . The momentum of the impulse chamber is delivered to the space craft through a piston, which exerts a constant thrust, T. The decelerating distance is then $L_{IC} = \frac{I_{IC}^2}{M_{IC} T}$, where T_{IC} is the deceleration time. Using the approximate relation Eq. (10), we obtain

$$L_{IC} = \frac{2T_{IC}\eta Y^{-1/6} \left(\frac{4\pi\sigma_T \Delta r}{3} \frac{r}{r} \right)^{1/3}}{\rho_s} \sim 0.86 T_{IC} Y_{GJ}^{-1/6} \text{ meters}. \quad (26)$$

$$\text{and } I_{sp} = \frac{\eta Y^{1/6} \left(\frac{4\pi\sigma_T \Delta r}{3} \frac{r}{r} \right)^{1/3}}{g \sqrt{\pi \Gamma_n}} \sim 4700 Y_{GJ}^{1/6} \text{ seconds} \quad (27)$$

for $r/\Delta r=10$. Equation (10) should be accurate for inertial fusion capsules that require an short risetime. We use Eqs. (7) and (25) to calculate the mass of the transmission line as a function of the current risetime. The results for several values of the yield are plotted in Fig. 24.

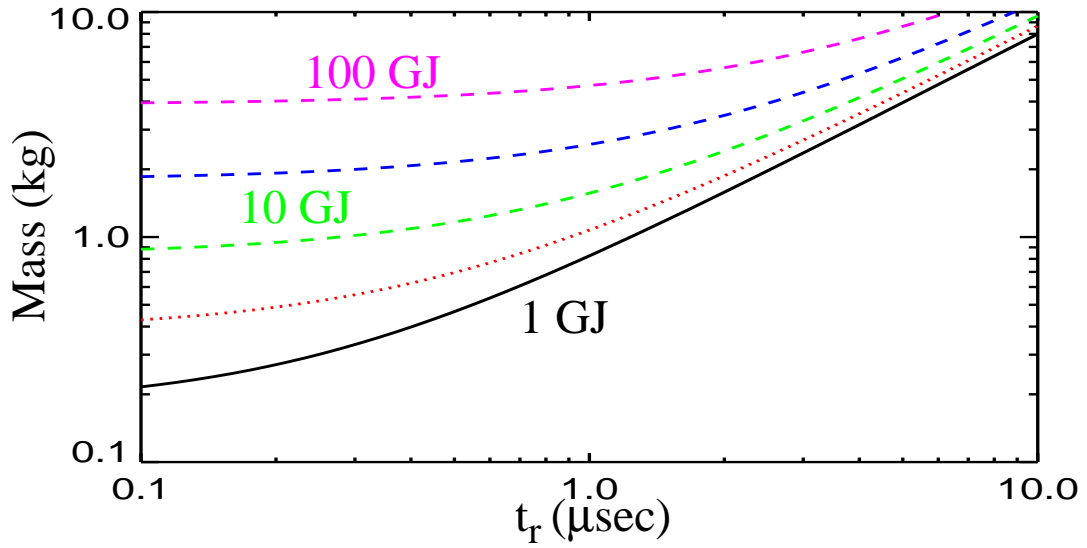


Fig. 24 The transmission line mass plotted as a function of the current risetime for several yields

The mass increases with yield because we have assumed that the transmission line radius scales according to Eq. (25). Deviations from Eq. (10) are apparent for the lower yield, becoming less important for high yields as would be expected. Equation (24) is used to calculate the specific impulse. The results are plotted in Fig. 25..

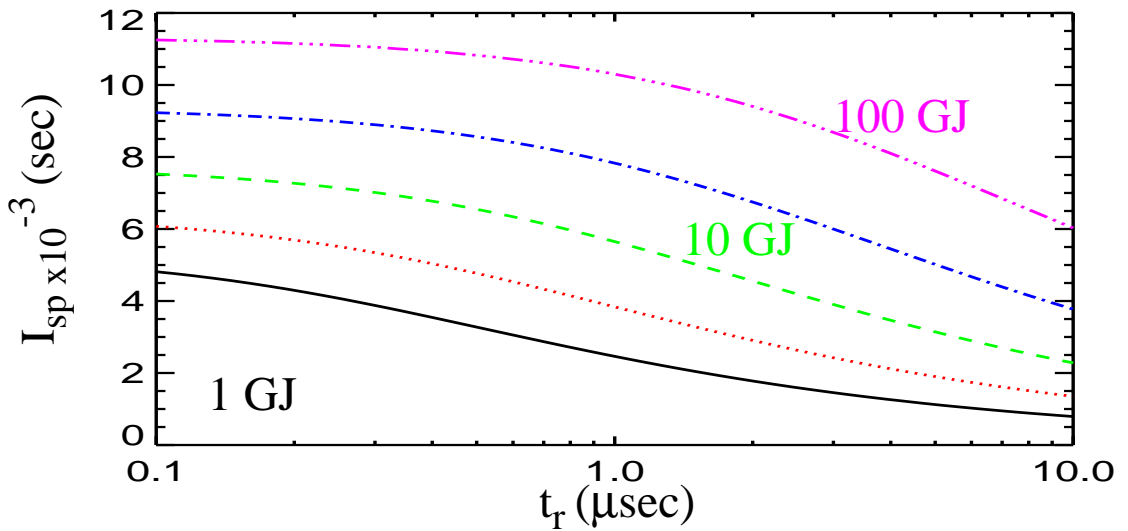


Fig. 25 The specific impulse is plotted as a function of the current risetime for several values of the yield

As can be seen, performance improves with yield and with shorter current risetimes. The results indicate that specific impulses greater than 4000 secs should be possible for a large range of yields and current risetimes. This should be compared to chemical rockets which produce a specific impulse of about 400 secs and nuclear thermal rockets which could produce about 800-1000 secs. Ion thrusters are capable of high specific impulse but at very low thrust. Consequently ion thrusters must burn for very long times (~years) to obtain high rocket exhaust velocities. As a comparison we have calculated the burn time required to obtain a velocity of 30 km/s for a space craft weighing 100 metric tons using the results shown in the last two figures. We have assumed an explosion at 1 second intervals. The results are shown in Fig. 26

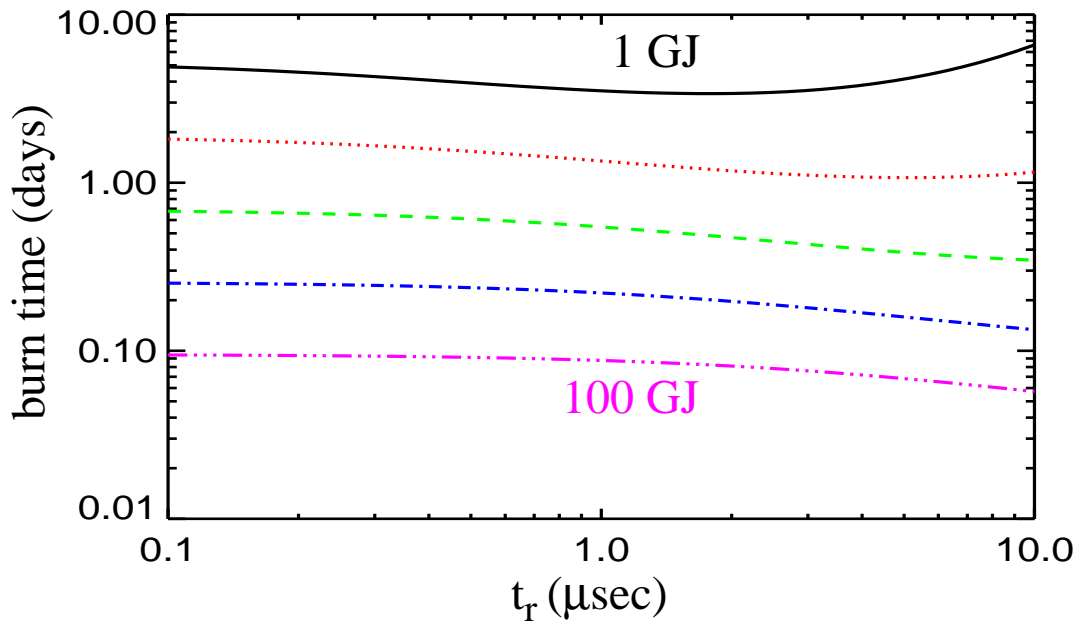


Fig. 26 The burn time required to reach 30 km/s for a 100 metric ton spacecraft

The burn times are a weak function of the pulse risetime but a strong function of the yield. Yields of about 10 GJ would result in a burn time of less than one day, and even 1 GJ results in a burn time much less than the mission time. Of course the burn time depends on the mass of the spacecraft. A fairly detailed design of the spacecraft will be needed to

accurately determine its mass. However, we can estimate the weight of the capacitors that would be needed. Dielectric materials⁴ have been developed that can store up to 4 kJ/kg. Approximately 20 MJ will be required to drive either a fusion capsule or a microfission capsule. Capacitors typically weigh 3-5 times as much as the dielectric due to electrodes and packing. Thus the capacitors would weigh approximately 5 metric tons, which is substantially less than the 100 metric tons assumed in the previous calculations

VI. Summary

We have investigated the issue of minimizing the mass of a transmission line which delivers current to a z pinch. We have shown that electrode thickness needed to provide sufficient inertia against the current induced magnetic field decreases strongly with radius and corresponds to very thin electrodes at the outer portion of the transmission line. We have performed experiments that indicate a minimum electrode thickness is required to avoid excessive resistive losses. These experiments indicate that 20 μ of mylar is sufficient to carry the current with acceptable resistive losses. This result indicates that a transmission line with a mass as little as 2 kg could be used for fusion energy applications. We have also analyzed the transmission line mass as a function of the current risetime to estimate specific impulse that could be obtained with a pulsed power driven fusion or fission rocket. The results indicate high values of the specific impulse (> 4000 secs) as compared to only 400 secs for a conventional chemical rocket.

Appendix

The effects of nonuniform heating of the transmission line are calculated in this appendix. Assume a disk transmission line of radius, r_T , with the explosive unit a distance z_T below as depicted in Fig. A1

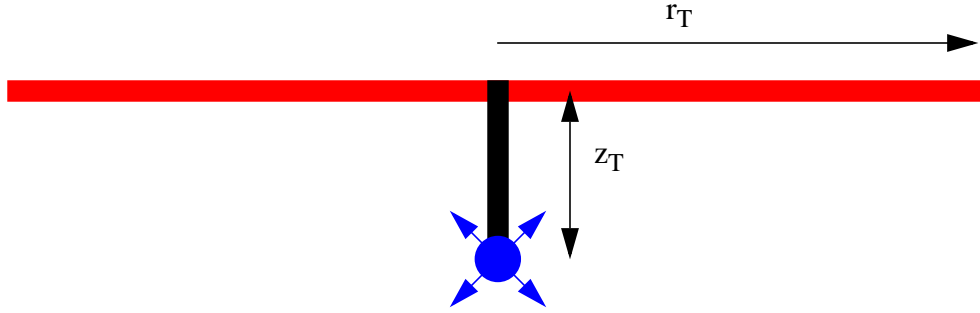


Fig. A1 Schematic of a disk transmission line with an explosive unit

Assume the explosive unit has a mass M_x and the transmission line has a mass M_T . Roughly 1/2 of the mass of the explosive unit is directed away from the transmission line (toward the rear of the spacecraft). The rearward momentum is

$$P_x = M_x \sqrt{\frac{2Y}{M_x}} \int \cos\theta \frac{d\Omega}{2\pi} = \frac{M_x}{4} \sqrt{\frac{2Y}{M_x}} \quad (\text{A1})$$

We assume that the energy flux from the explosion is isotropic and is thus given by the formula

$$F_E(x) = \frac{Y}{4\pi r_T^2} \frac{x_T}{(x^2 + x_T^2)^{3/2}} \quad (\text{A2})$$

where $x=r/r_T$ and $x_T=z_T/r_T$. The mass flux is similarly

$$F_M(x) = \frac{M_x}{4\pi r_T^2} \frac{x_T}{(x^2 + x_T^2)^{3/2}} \quad (\text{A3})$$

The mass flux adds to the areal density of the transmission line which we assume to be $\Gamma = 2\Gamma_n$ to account for two electrodes. The characteristic expansion velocity at each radius along the transmission line is then

$$v_x = \left(\frac{2F_E(x)}{F_M(x) + \Gamma} \right)^{1/2} \quad (\text{A4})$$

We assume that the impulse chamber redirects this expanding plasma toward the rear with an average direction cosine $\zeta_n = \overline{\cos\theta}$. The rearward momentum is then

$$P_T = \zeta_n \int_0^1 2\pi r_T^2 x dx \{2F_E(x)(F_M(x) + \Gamma)\}^{1/2} \quad (\text{A5})$$

The average rearward velocity is $\bar{v} = \frac{P_x + P_T}{M_x + M_T}$. We define $\eta = \bar{v} \sqrt{\frac{M_T}{2Y}}$ and $\mu = \frac{M_x}{M_T}$

We obtain the expression

$$\eta = \frac{1}{(1 + \mu)} \left\{ \frac{\sqrt{\mu}}{4} + \zeta_n \int_0^1 x dx \left\{ \frac{x_T}{(x_T^2 + x^2)} \left(1 + \frac{\mu x_T}{4(x_T^2 + x^2)} \right) \right\}^{1/2} \right\} \quad (\text{A6})$$

Using $\zeta_n = 1$, the results are plotted in Fig. A1 for $\mu=0$ and $\mu=0.1$, which was found to produce a maximal value of η . Clearly adding mass to the explosive unit has a minimal effect and one can expect $\eta \approx \frac{1}{2}\zeta_n$.

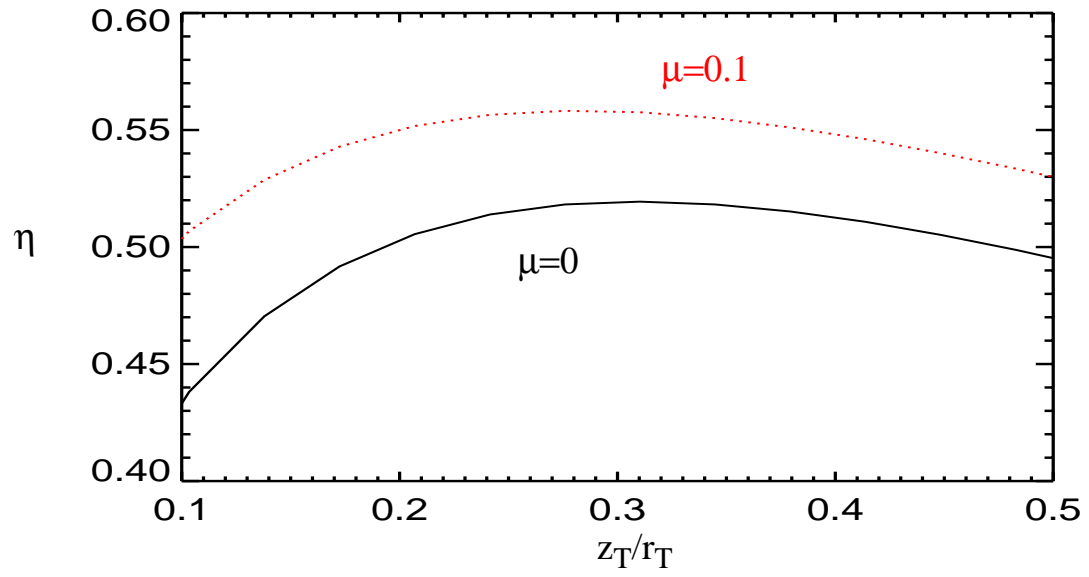


Fig. A2 The specific impulse coefficient η is plotted as a function of z_T/r_T for two values of $\mu=M_x/M_T$.

References

- 1 J. Lash, G.A. Chandler, G. Cooper, M.S. Derzon, M.R. Douglas, D. Hebron, R.J. Leeper, M.K. Matzen, T.A. Mehlhorn, T.J. Nash, R.E. Olson, C.L.Ruiz, T.W.L. Sanford, S.A. Slutz, D.L. Peterson, and R.E. Chrien, “The Prospects for High Yield ICF with a Z-Pinch Driven Dynamic Hohlraum”, Proceedings of Inertial Fusion Science and Applications 99, Bordeaux, FR, Sept. 1999, edited by C. Labaune, W.J. Hogan, K.A. Tanaka (Elsevier, Paris, 2000), Vol. I, p. 583
- 2 S.A. Slutz, M.R. Douglas, J.S. Lash, R.A. Vesey, G.A. Chandler, T.J. Nash, and M.S. Derzon, Phys. Plas. 5, 1673
- 3 F. J. Dyan, Physics Today, 21, 41, 1968
- 4 Masarakis private communication

distribution

- 10 Prof. Per F. Peterson
Dept. of Nuclear Engineering
4111 Etcheverry
University of California
Berkeley, CA 94720-1730
- 1 Dr. Robert R. Peterson
Dept. of Nuclear Engineering and Engineering Physics
Fusion Technology Institute
University of Wisconsin
1500 Engineering Drive
Madison, WI 53706
- 3 Cornell University
Laboratory of Plasma Studies
Attn: D. A. Hammer
B. R. Kusse
J. B. Greenly
369 Upson Hall
Ithaca, NY 14853
- 5 Lawrence Livermore National Laboratory
Attn: John Perkins L-637
B. G. Logan L-481
J. Hammer L-018
John Lindl L-039
M. Tabak L-015
A. Toor L-041
P.O. Box 5511 7000 East Ave
Livermore, CA 94550
- 2 Imperial College
Attn; M. Haines
G. Chittenden
South Kensington, London
SW72BZ, United Kingdom
- 1 Institute für Kernphysik
Attn: D. H. H. Hoffmann
Strahlungs-und Kernphysik
TU Darmstadt, Karolinenplatz
D 64289 Darmstadt, Germany
- 1 Universite Paris SUD
Attn: C. Deutch
Laboratoire de Physique des Gas et des Plasmas
BAT 210 LP CEP R-91405

Orsay, France

1 University of Nevada Reno
Attn: B. Bauer
Department of Physics, Reno, NV 89557

2 Los Alamos National Laboratories
Attn: D. Peterson X-PA
R. Bowers X-TA
Los Alamos, NM 87545

1 Weizman Institute of Physics
Attn: I. Maron
Department of Physics
Rehovot 76100, Israel

1 Lawrence Berkeley National Laboratory
Attn: R. O. Bangerter
1 Cyclotron Rd
Berkeley, CA 94720

1 University of California Davis
Attn: J. DeGroot
Dept. of Applied Science
Rm 228 Walker Hall
Davis, CA 95616

1	MS-0188	4523	C.E. Meyers
1	MS-0151	16000	G. Yonas
1	MS-0736	6400	T. E. Blejwas
1	Ms-0865	1900	D. Cook
30	MS-1188	9500	C. Olson
1	MS-1190	1600	J. Quintenz
1	MS-1191	1670	M. Sweeney
1	MS-1181	1610	J. Asay
1	MS-1178	1630	D. Bloomquist
1	MS-1194	1640	D. McDaniel
1	MS-1194	1612	C. Deeney
1	MS-1194	1644	W. Stygar
1	MS-1191	1600	K. Matzen
1	MS-1193	1673	J. Porter
1	MS-1186	1674	T. Mehlhorn
1	MS-1196	1677	J. Bailey
1	MS-1193	1673	M. Cuneo
1	MS-1186	1674	M. P. Desjarlais
20	MS-1186	1674	S. Slutz

1	MS-1186	1674	R. Vesey
1	MS-1196	1677	R. Leeper
1	MS-1196	1677	G. Chandler
1	MS-0839	16000	M. Derzon
1	MS-1196	1677	R. E. Olson
1	MS-1196	1677	T. Sanford
1	MS-9018	8945-1	Central Technical Files
2	MS-0899	9616	Technical Library
1	MS-0612	9612	Review and Approval Desk For DOE/OSTI